Наносистеми, наноматеріали, нанотехнології
Nanosystems, Nanomaterials, Nanotechnologies
2015, т. 13, № 1, сс. 85–97

PACS numbers: 07.78.+s, 61.05.J-, 61.05.jd, 61.43.Dq, 68.37.Lp, 68.55.jd, 87.64.Ee

Different Electron-Scattering Mechanisms' Contribution to the Formation of the Amplitude Contrast of Electron-Microscopic Images

M. Yu. Bobyk, V. P. Ivanitsky, M. M. Ryaboshchuk, and O. Ya. Svatyuk

National University of Uzhhorod,
Narodna Place, 3,
88000 Uzhhorod, Ukraine

A new method of experimental determination of the amplitude contrast value of electron-microscopic images for amorphous materials is suggested. The mathematical relations for calculating the contributions of different mechanisms of electron scattering by the object under study to the contrast on the basis of the relevant electron-diffraction patterns are obtained. The shares of contribution of elastically coherently, elastically incoherently, and inelastically scattered electrons to the contrast are determined experimentally for the amorphous $As_{40}Se_{60}$ films.

Запропоновано новий метод експериментального визначення амплітуди контрастного значення електронно-мікроскопічних зображень для аморфних матеріалів. Були одержані математичні співвідношення для розрахунку внесків різних механізмів розсіювання електронів на досліджуваному об'єкті в контраст на основі відповідних електронограм. Для аморфних плівок $As_{40}Se_{60}$ були знайдені експериментально частки внесків пружньо когерентно, пружньо некогерентно та непружньо розсіяних електронів у контраст.

Предложен новый метод экспериментального определения амплитуды контрастного значения электронно-микроскопических изображений для аморфных материалов. Были получены математические соотношения для расчёта вкладов различных механизмов рассеяния электронов на изучаемом объекте в контраст на основе соответствующих электронограмм. Для аморфных плёнок $As_{40}Se_{60}$ были найдены экспериментально доли вкладов упруго когерентно, упруго некогерентно и неупруго рассеянных электронов в контраст.

Key words: electron microscopy, electron diffraction, amplitude contrast, amorphous material, morphology of films, microstructure.

(Received 27 February, 2015)

1. INTRODUCTION

The bright field-imaging mode is the most common mode of operation in the transmission electron microscopy. The results of such electron microscopy (EM) experiments are fixed in a form of the two principal complementary sources of information: the electron diffraction patterns (*i.e.* electronograms, diffractograms, microelectronograms, nanoelectronograms) and the EM images of different areas of the object under study.

In most cases, the subject of analysis of the EM images of crystalline materials is the diffraction contrast elements. They arise due to the coherently scattered electrons that interfere making the corresponding diffraction pattern. Therefore, when studying the crystal microstructure, the analysis of the relevant EM images and that of the electronograms are closely related [1].

The microstructure and the nanostructure of the amorphous specimens are studied in accordance with their EM images only. In this case, it is assumed that in such images the amplitude contrast is mainly formed [2]. It is assumed here, as a rule, that inhomogeneities of the EM images are determined mainly by the difference in the thicknesses or masses of the local areas of the specimen under study [3]. In the experimental studies, such contrasts in the EM images are called the 'mass–thickness' contrast and describe them mainly qualitatively, *i.e.* determine the image homogeneity or heterogeneity, provide qualitative and several quantitative geometric parameters of heterogeneities. Such a theoretical approach to the analysis of the amplitude contrast of amorphous materials is very limited and does not take into account a number of factors that affect essentially the processes of the EM image formation. The principal of the above factors is the character of the spatial distribution of all the waves scattered by the specimen under study.

In general, for each chemically and structurally homogeneous local area of the amorphous specimen, the electron wave (or the electron flux) intensity that forms the EM image of this area could be set by a simple relation [3]:

$$I = I_0 \exp(-Qd), \tag{1}$$

where Q is the parameter that characterizes the ability of this area to scatter electrons outside the aperture diaphragm. Therefore, finding the relationship between the electron beam intensity at a certain EM image point with integral scattering property Q of the relevant local

area of homogeneous specimen and the geometric thickness d of this area makes a ground of the amplitude contrast analysis. If one reduces the intensity I in (1) to a single atom and to the unit intensity of the incident beam I_0, then the presence of variation of the scattering property of atoms for various areas of the object under study and their thicknesses will be definitive for production of the EM contrast. Scattering property variations could arise due to the differences in the structure of these areas, *i.e.* different atomic density, chemical composition, structure of the short-range and medium-range order, nanoporosity, *etc*. Therefore, it is advisable to have the experimental methods of determining contribution of the differences of each of above parameters of the amorphous material structure into the amplitude contrast. In this paper, we suggest one of the possible approaches to the solution of such problem of the applied electron microscopy. It is based on the fact that, for each amorphous material, the contrast observed in EM is formed by electrons scattered by the atoms of the specimen under study according to the three physical mechanisms, *i.e.* the elastic coherent, the elastic incoherent and the inelastic ones.

2. EXPERIMENTAL TECHNIQUE

Thin amorphous films were obtained by a method of discrete thermal evaporation of the $As_{40}Se_{60}$ glass with vapour condensation onto the substrate made of the NaCl single crystal. The substrates were not heated and were kept at the room temperature. Condensation rate was of 5–7 nm/s. Condensed film thickness was of 50–60 nm. The specimens for the EM studies were prepared according to the standard technique of substrate dilution in the distilled water with film material trapping by the golden grids. As for the use of the copper grids, this resulted in the uncontrolled fast changes of the film atomic structure during the EM experiments not allowing their reliable diffractograms to be obtained.

The EM studies of the amorphous $As_{40}Se_{60}$ films were carried out using the transmission electron microscope JEM-2010 at the 100 kV accelerating voltage. The images and electronograms were detected by the Catan Ultrascan 4000SP CCD camera and processed by the computer software.

The EM studies included several stages.

1. The general electronogram of the amorphous film was detected in the diffraction mode at one picture. Then, the aperture diaphragm was introduced 'cutting out' the central beam together with the adjacent area of scattered electrons and the second picture was taken fixing the diaphragm location against the electronogram background. Comparing these two pictures enabled us to determine the scattering angle value θ_a that corresponds to the edges of the aperture diaphragm.

2. The microstructure and the nanostructure of the specimens were studied in the common light field mode. Such studies allowed the local areas to be found in the amorphous film differing by their microstructure.

3. The microstructurally homogeneous areas of the specimen were selected by the microdiffraction diaphragm and their microdiffraction patterns were detected. Microdiffractograms of 5–7 different areas were fixed in the same experiment for the same specimen. The data obtained were compared with each other and then the average microdiffractogram of the areas under study was calculated using the computer program. Further computer processing of this microdiffractogram allowed it to be presented in a form of the intensity of electrons scattered by the local area as a function of scattering angle, $I(\theta)$. The function $I(\theta)$ was determined reliably in the relative units within the range of scattering angle variation from 2 mrad to 30 mrad with the 0.3 mrad discretization step. The scattering angle (θ) axis scale was determined with the help of the 'embedded' thin golden films.

The normalizing factor α is a significant parameter of electronogram and microdiffractogram processing at the EM studies. Having found its value, one could easily transit from the relative to the absolute units of electron scattering intensity. This allows the correct and reliable comparison of diffractograms of the amorphous films of different chemical compositions to be done as well as the reliable calculations of electron fluxes forming the EM images of the objects under study to be carried out on their basis. We have determined the normalizing factor and divided the total intensity $I(\theta)$ into the elastic component and the incoherent background using the method described in [4]. The initial tabulated values of atomic scattering amplitudes $F(\theta)$ were taken for calculations from tables quoted in [5].

3. CONTRIBUTION OF DIFFERENT SCATTERING TYPES INTO THE CONTRAST

It has been shown [6] that the contrast between the EM images of the two local areas of the object under study could be conveniently found as

$$K = (\Phi_1 - \Phi_2)/\Phi_1 = 1 - \Phi_2/\Phi_1 = \Delta/\Phi_1, \qquad (2)$$

where Φ_1 and Φ_2 are the integral fluxes of the electron waves scattered by the two local areas outside the aperture diaphragm (it is assumed here that $\Phi_1 \geq \Phi_2$).

In order to find experimentally the flux Φ, one has to integrate the intensity $I(\theta)$ (see Fig. 1) over the entire space beyond the aperture diaphragm used to obtain the EM image patterns. An arrow in Figure 1

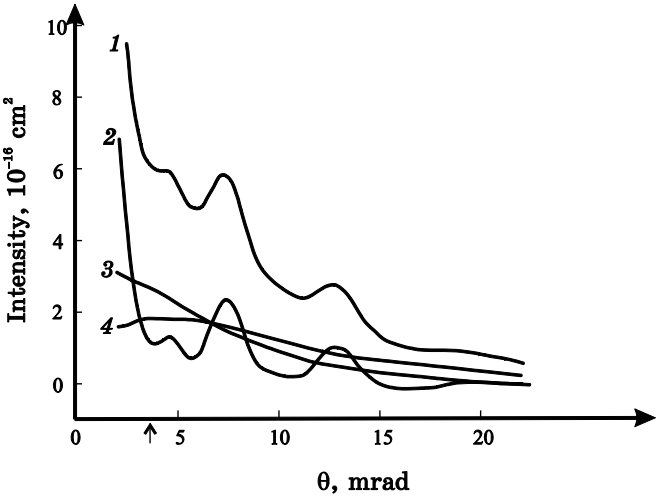

Fig. 1. Microdiffractogram of the 60 nm thick amorphous $As_{40}Se_{60}$ film (curve *1*) with selected different scattering components: the elastic coherent (*2*), the elastic incoherent (*3*) and the inelastic (*4*) ones. The intensities are reduced to a single scattering atom.

indicates the scattering angle value that corresponds to the aperture diaphragm boundary. Accordingly, integration should be carried out within the scattering angle range $\theta_a < \theta < \theta_{max}$, where θ_{max} is the boundary scattering angle value up to which the intensity $I(\theta)$ was measured. In these conditions, one may write for each local area:

$$\Phi = 2\pi \int_{\theta_a}^{\theta_{max}} I(\theta) \sin\theta d\theta \,. \tag{3}$$

According to Figure 1, the integral intensity $I(\theta)$ for each local area could be resolved into components, *i.e.* into the elastic coherent $I_k(\theta)$, the elastic incoherent $I_e(\theta)$ and the inelastic $I_n(\theta)$ ones. Then, relation (3) takes a form:

$$\begin{aligned} \Phi &= 2\pi \int_{\theta_a}^{\theta_{max}} I_k(\theta) \sin\theta d\theta + 2\pi \int_{\theta_a}^{\theta_{max}} I_e(\theta) \sin\theta d\theta + 2\pi \int_{\theta_a}^{\theta_{max}} I_n(\theta) \sin\theta d\theta = \\ &= \Phi_k + \Phi_e + \Phi_n, \end{aligned} \tag{4}$$

where Φ_k, Φ_e, Φ_n are the electron fluxes of the relevant electron waves scattered beyond the aperture diaphragm. Obviously, it is expedient to determine quantitatively the amplitude contrast from (2) by analysing each of the above-mentioned fluxes separately.

To solve the problem of the quantitative analysis of the amplitude EM contrast on the basis of expressions (1)–(4), one has to use approx-

imations adequate to the real conditions.

The idea of one of approximations is that the EM image is considered a result of 'imposition' of intensities of the electron scattering by a great number of atoms. Therefore, formation of such image could be mathematically set in a form of summating all the electron waves scattered by separate atoms according to the laws specific both for the coherent and incoherent electron waves. The procedure of summation could be substantially simplified by introducing the electron scattering parameters averaged over a certain macrovolume of the specimen into consideration. Obviously, this approximation confidence will be determined by the rules of averaging.

Let us analyse the contribution of different types of electron scattering by the object under study to the EM contrast.

4. ELASTIC INCOHERENT SCATTERING

Consider the first component of the electron flux Φ_e that is due to the processes of incoherent scattering of the probing beam electrons by the atoms of the specimen under study. The intensity of this component is equal to the sum of effects of independent scattering by separate atoms from the selected local area. The spatial distribution of the intensity of the electron beam scattering by a single i-th atom is defined by its atomic factor $F_i^2(\theta)$, where $F_i(\theta)$ is the amplitude of electron scattering by the above atom. Therefore, the intensity $I_e(\theta)$ of elastic incoherent scattering by a certain local area of the specimen of the complex chemical composition could be determined via the atomic factor $F^2(\theta)$ averaged over this area volume:

$$I_e(\theta) = NF^2(\theta) = \sum_{i=1}^{N} F_i^2(\theta) = N \sum_{j=1}^{m} c_j F_j^2(\theta) , \qquad (5)$$

where N is the number of atoms included into the local area, m is the number of different chemical elements in the local area, c_j are the relative shares of different chemical elements of the local area. Thus, variations of intensity of the elastic incoherent electron scattering by different local areas will be determined by the changes in the number of atoms N and relative concentrations c_j of different chemical elements in these local areas. The flux Φ_e due to the above processes could be consequently calculated from (4) as:

$$\Phi_e = 2\pi N \int_{\theta_a}^{\theta_{max}} F^2(\theta) \sin\theta d\theta . \qquad (6)$$

Let us analyse the process of formation of the flux Φ_e in more detail. To do this, we will introduce the following approximation: the whole volume of the specimen local area will be considered uniformly filled

with the atoms having the average atomic density ρ_0. For the substances with a complex chemical composition, this density is a sum of the partial atomic densities of different chemical elements ρ_{0i}, *i.e.*

$$\rho_0 = \sum_{i=1}^{m} \rho_{0i} , \tag{7}$$

where $\rho_{0i} = c_i\rho_0$. In these conditions, $\rho_{0i}S_l dx$ atoms of the i-th chemical element will take part in the electron scattering inside the local area volume with the thickness dx, where S_l is the cross section of the local area of the object under study. In such a case, dn_i electrons will be elastically scattered by the atoms of a certain i-th chemical element beyond the aperture diaphragm at the electron beam transmission through this specimen area. This quantity ratio to the total number of not yet scattered electrons n will be as follows:

$$\frac{dn_i}{n} = -\frac{\sigma_{ei}\rho_{0i}S_l dx}{S_l} = -\sigma_{ei}\rho_{0i}dx , \tag{8}$$

where σ_{ei} is the cross section of the elastic electron scattering by the atoms of a certain i-th chemical element beyond the aperture diaphragm.

The further theoretical consideration of the electron scattering processes in the objects with a complex chemical composition should be carried out having introduced the elastic scattering cross section per a single atom averaged over all the chemical elements in the local area $\bar{\sigma}_e$. In our opinion, such procedure could be correctly realized by applying the physical essence of the elastic incoherent scattering process, *i.e.* the total electron scattering intensity is equal to the sum of independent electron scatterings by atoms of different chemical elements. Then, taking into account (8), we have:

$$\frac{dn}{n} = \sum_{i=1}^{m} \frac{dn_i}{n} = -\sum_{i=1}^{m} \left(\sigma_{ei}\,\rho_{0i}\right) dx . \tag{9}$$

Taking into account relation (7), the derived expression could be written as follows:

$$\frac{dn}{n} = -\sum_{i=1}^{m} \left(\sigma_{ei}c_i\,\rho_0\right) dx = -\rho_0 \sum_{i=1}^{m} \left(c_i\,\sigma_{ei}\right) dx . \tag{10}$$

It follows from the last equation that it is expedient to define the elastic scattering cross section per a single atom averaged over all the chemical elements of the specimen $\bar{\sigma}_e$ as:

$$\bar{\sigma}_e = \sum_{i=1}^{m} c_i\sigma_{ei} . \tag{11}$$

Solving a simple differential equation (10) with the assumed defini-

tion (11) gives the dependence of the number of electrons not scattered beyond the aperture diaphragm on the thickness of the local area x passed by them:

$$n = n_0 \exp\left(-\bar{\sigma}_e \rho_0 x\right), \tag{12}$$

where n_0 is the number of probing beam electrons falling onto the selected area.

Thus, the electron beam flux retarded by the aperture diaphragm and not involved in the formation of the EM image of the local specimen area due to elastic incoherent scattering will be determined by the quantity $n_0 - n$ at the exit from this local area. Therefore, one may write down that this flux is equal to

$$\Phi_e = \Phi_0 \left[1 - \exp(-\bar{\sigma}_e \rho_0 d)\right], \tag{13}$$

where Φ_0 is the value of the probing beam electron flux at the object.

Comparison of this relation with equation (1) shows that the scattering property of the object area Q due to the elastic incoherent scattering is determined by the product of the three main parameters: the averaged cross section of elastic electron scattering by the local area atoms beyond the aperture diaphragm $\bar{\sigma}_e$, the average atomic density of the specimen local area ρ_0 and the geometric thickness of this area d. In the applied electron microscopy of amorphous substances with complex chemical composition, any of the above parameters may vary when going from one local area to another, giving, thus, its own contribution to the EM image contrast. In this case, the $\bar{\sigma}_e$ variation occurs due to that of the local area chemical composition, ρ_0 variation takes place due both to that of the chemical composition and to the presence of different continual heterogeneities in the local areas in a form of nanopores, while d variation is due to the specific features of the specimen surface topology.

5. ELASTIC COHERENT SCATTERING

The elastic coherent scattering I_k is a second by its role in forming the amplitude contract of the EM images of the amorphous substances. It reflects the diffraction effects related to the interaction and interference of electron waves scattered by different atoms. The value and the spatial distribution of the elastic coherent scattering are determined by the parameters of the short-range and medium-range orders of disordered atomic network. Therefore, the contribution of the coherent scattering to the EM image formation is sometimes called the 'structural' contrast.

The structural factor $S(\theta)$ of the intensity distribution of the coher-

ent elastic scattering by the amorphous object beyond the aperture diaphragm is a basic characteristic that defines its character [7]. Therefore, one may state with quite high accuracy that the amplitude contrast of the EM images due to the elastic coherent electron scattering will be expressly determined by the $S(\theta)$ function differences beyond the aperture diaphragm for different local specimen areas. Accordingly, the variations of the short-range and medium-range order parameters of the amorphous substance atomic network at the transitions from one local area to other ones will be responsible for its appearance.

Within the framework of the approximations assumed above, the distribution of the intensity I_k of the elastic coherent electron scattering by the amorphous substance with complex chemical composition could be set as follows [8]:

$$I_k(\theta) = NF^2(\theta)[S(\theta) - 1]. \tag{14}$$

As shown above, the function $S(\theta)$ is easily determined experimentally by detecting electronograms from the object areas under study. From the viewpoint of contrast formation, we are interested in the difference in electron scattering by different local areas of the same specimen. The minimal dimensions of such local areas in modern nanomaterials and nanosystems are of the units of nanometres. Therefore, to use relation (14), one has to apply the electronographic methods that allow separate diffractograms to be obtained from the specimen areas with nanometric size. The electron diffraction method with strong electron beam focusing [9, 10] complies with these requirements. It allows the atomic structure of the nanoareas with size more than 5 nm to be studied. Such specimen areas could be exactly distinguished in the EM image.

Having the nanoelectronograms from different local nanoareas of the object obtained in the strong focusing mode according to the technique suggested above, one might calculate their structural factors $S(\theta)$ and, accordingly, obtain the spatial distributions of the coherent elastic electron scattering from these local areas from relation (14). As a result, now, it is possible to calculate the contribution of the differences in atomic structure of amorphous specimens into the EM image contrast in a form of a relevant flux Φ_k:

$$\Phi_k = 2\pi N \int_{\theta_a}^{\theta_{\max}} F^2(\theta)\left[S(\theta) - 1\right]\sin\theta d\theta . \tag{15}$$

It should be noted here that the function $S(\theta)$ must be exactly determined from the nanoelectronogram in the large-angle electron scattering region. In this region, the nanoelectronograms have low intensity, and this may affect considerably the result of the contrast analysis.

6. INCOHERENT SCATTERING

When analysing the EM image contrast one has also to take into account the electron energy losses in the specimen, *i.e.* to take into account the inelastic scattering as well. By its nature, it is incoherent and depends on the number of atoms in the area under study.

Theoretical principles of the influence of inelastic electron scattering on the EM image contrast formation are much more complicated as compared to those on case of elastic scattering. This is due to a number of reasons [11].

1. Such scattering is very sensitive to the change in the state of the atomic electron orbits and electron density at large distances from atomic nuclei. Therefore, the scattering characteristics determined for certain atoms strongly differ from those for the case of the inelastic atom scattering in the condensed matter.

2. Unlike the elastic scattering, inelastic electron scattering differs drastically from the inelastic X-ray Compton scattering.

3. A share of inelastic scattering is especially large in the low s region, where its intensity I_n may exceed that of the elastic scattering by several orders of magnitude. Only this region corresponds to the aperture diaphragm transmission and plays an important role in the amplitude EM contrast formation.

Simultaneous and complex action of the above factors stipulates traditionally preferable use of experimental methods of determining the spatial intensity distribution $I_n(\theta)$ in order to consider inelastic scattering in the applied electron microscopy and electronography [12]. Knowing this distribution found using the above-mentioned technique, one may calculate the electron flux that is responsible for the formation of the inelastic scattering contribution into the contrast:

$$\Phi_n = 2\pi N \int_{\theta_a}^{\theta_{max}} I_n(\theta) \sin\theta d\theta \,. \qquad (16)$$

Note that, in the applied electron microscopy, the $I_n(\theta)$ component of intensity includes also the 'parasite' background electron scattering by the residual gas molecules in the microscope column, at the diaphragm edges, *etc*.

7. RESULTS AND THEIR ANALYSIS

Figure 1 presents the distributions of the integral electron scattering intensity I (curve 1) and its components as the functions of the scattering angle for the amorphous $As_{40}Se_{60}$ film. The above intensities correspond to the scattering by a single 'averaged' atom of the specimen.

The scattering angle value $\theta_\alpha = 3.8$ mrad corresponds to the location of the aperture diaphragm edges when obtaining the EM pictures in our experiments. Based on these experimental data and using relations (6), (15) and (16), we have determined the relative fluxes Φ_{e1}, Φ_{k1}, Φ_{n1} of electrons scattered beyond the aperture diaphragm according to different mechanisms per a single averaged atom of the specimen under study: $\Phi_{e1} = 6.6 \cdot 10^{-6}$, $\Phi_{k1} = 5.1 \cdot 10^{-6}$, $\Phi_{n1} = 9.1 \cdot 10^{-6}$. These quantitative data indicate that, in the 50–60 nm amorphous thick $As_{50}Se_{50}$ films, almost a half of the scattered electrons appear to be scattered beyond the aperture diaphragm. At the same time, approximately same number of electrons are scattered elastically coherently and elastically incoherently.

The above relations were obtained in the single electron-specimen scattering approximation. However, the total intensity $I(s)$ involves a large part of multiply scattered electrons, *i.e.* those, for which the number of interactions with atoms during their passing the specimen exceeds a unit but is less than that necessary to describe the scattering processes by a normal Gauss distribution. The latter holds true in case of a multiple scattering.

A strict account of the multiple scattering influence using known theoretical expressions is an unsolvable problem until now [11]. Complexity of its solution is related to the fact that in each scattering act one of the three above analysed mechanisms of electron interaction with the specimen under study could be realized. For example, triply scattered electron may take part in the elastic coherent, elastic incoherent, and inelastic scattering in the three serial interactions with the specimen atoms. The studies of such processes and their contributions to the EM contrast are an independent problem of the theory and practice of the modern electron microscopy. However, taking into account the high intensity of the multiple electron scattering by the objects with a thickness of several dozens of nanometres [13], one may state that for such specimens the fluxes Φ_k, Φ_e, and, especially, Φ_n include also a substantial part of the above multiple scattering. In our opinion, only the multiple scattering contribution stipulates such a large part of electrons being incoherently scattered by the specimens under study beyond the aperture diaphragm.

If the heterogeneities of any origin are present in the specimen under study, then, the relevant fluxes Φ_k, Φ_e, Φ_n will differ from each other. Such differences will cause the appearance of the relevant contrasts between the different areas of the heterogeneous object in the EM image. Using the method suggested above and the above relations, one may find on the quantitative analysis level the real nature of nanoheterogeneities present in the amorphous objects. If one takes into account that the EM pictures reliably demonstrate the 2–3% contrast values, then for their appearance, the above fluxes Φ_k, Φ_e, Φ_n (or their

sum) from the two local areas of the heterogeneous specimen must differ just by this value.

8. CONCLUSIONS

The electron wave intensity distribution in the plane of formation of the EM image amplitude contrast is due to the probing electron beam scattering by the object and consists of three main parts. The first part is determined by the elastic incoherent scattering $I_e(s)$ and equals to the sum of scattering effects related to each separate atom independently of any other atoms. The second part is the elastic coherent scattering $I_k(s)$ that causes formation of the diffraction pattern from material. And the third intensity, $I_n(s)$, results from the inelastic electron scattering processes. The spatial distribution and the intensity $I_e(s)$ are determined by the averaged cross section of electron scattering by atoms of the specimen under study, its average atomic density, and geometric thickness. It seems expedient to calculate the coherent scattering contribution $I_k(s)$ via the experimental structural factor defined by the short-range and medium-range orders of the atomic network in the object under study. The inelastic scattering component $I_n(s)$ could be found from the results of the diffraction experiments in the course of normalizing the intensity of the coherent electron scattering by the specimen under study. Based on the intensities found, one may calculate the electron fluxes that form the EM images of different local areas of the specimen under study and find the real physical and chemical nature of its nanoheterogeneities on the quantitative level.

REFERENCES

1. B. Fultz and J. Howe, *Transmission Electron Microscopy and Diffractometry of Materials* (Heidelberg: Springer: 2007).
2. P. Hawkes, *The Beginnings of Electron Microscopy* (Orlando: Academic Press: 1985).
3. D. B. Williams and C. B. Carter, *Transmission Electron Microscopy: A Textbook for Materials Science* (New York: Springer: 2009).
4. N. G. Nakhodkin, A. P. Bardamid, and A. I. Novoselskaya, *Thin Solid Films*, **112**, No. 2: 267 (1984).
5. R. Herman and R. Hofstadter, *High-Energy Electron Scattering Tables* (Stanford: Stanford University Press: 1966).
6. M. Yu. Bobyk, E. I. Borkach, V. P. Ivanytskyy, and V. I. Sabov, *Nanosistemi, Nanomateriali, Nanotehnologii*, **10**, No. 3: 423 (2012) (in Ukrainian).
7. B. E. Warren, *X-Ray Diffraction* (New York: Dower: 1990).
8. A. C. Wright, *J. Non-Cryst. Solids*, **123**, No. 1: 129 (1990).
9. Y. Hirotsu, M. Ishimaru, T. Ohkubo, T. Hanada, and M. Sugiyama, *J. Electron*

Microscopy, **50**, No. 6: 435 (2001).
10. W. McBride, D. J. H. Cockayne, and K. Tsuda, *Ultramicroscopy*, **94**, Nos. 3–4: 305 (2003).
11. L. Reimer and H. Kohl, *Transmission Electron Microscopy: Physics of Image Formation* (New York: Springer: 2008).
12. Z. L. Wang, *Elastic and Inelastic Scattering in Electron Diffraction and Imaging* (New York: Plenum Press: 1995).
13. H. Lipson and S. G. Lipson, *J. Appl. Cryst.*, **5**, No. 2: 239 (1972).